NASA
Technical
Paper
2496

July 1985

Effect of Speed and Press Fit on Fatigue Life of Roller-Bearing Inner-Race Contact

Harold H. Coe and
Erwin V. Zaretsky

NASA

NASA
Technical
Paper
2496

1985

Effect of Speed and Press Fit on Fatigue Life of Roller-Bearing Inner-Race Contact

Harold H. Coe and
Erwin V. Zaretsky

Lewis Research Center
Cleveland, Ohio

National Aeronautics
and Space Administration

Scientific and Technical
Information Branch

Summary

An analysis was performed to determine the effects of inner-ring speed and press fit on the rolling-element fatigue life of a roller-bearing inner-race contact. The effects of the resultant hoop and radial stresses on the principal stresses were considered. The maximum shear stresses below the Hertzian contact were determined for typical inner rings with outer diameters of 51 and 127 mm (2.0 and 5.0 in) and inside- to outside-diameter ratios of 0.50 to 0.92 run at speeds of 500 and 2000 rad/sec (4800 and 19 000 rpm) with a loading of 0.7, 1.4, and 2.1 GPa (100, 200, and 300 ksi) Hertz stress. The ensuing life analysis, by using these shear stresses, showed that for some conditions the combined effects of speed and press fit can reduce the rolling-element fatigue life of the inner ring by more than 90 percent from that obtained by using conventional life calculations. Of this reduction, the centrifugal effects can account for over 80 percent at the higher speed. At the lower speed, where the life reduction may be only 50 percent, the press fit can account for 80 percent of the change. The depth of the maximum shear stress remained virtually unchanged from the conventional (Hertz stress only) calculations.

Introduction

It has been recognized for quite some time that a residual compressive stress near the surface of contact improves the fatigue life of that surface (refs. 1 and 2). Residual stresses can be developed from a number of processing operations (ref. 3). The effect of residual stresses induced by shot peening the surfaces of AISI 9310 gear teeth is shown experimentally and analytically in reference 4. Although the analysis in reference 4 was done for spur gears, it is also applicable to roller-bearings whenever residual stresses are present. However, if residual stresses can affect the fatigue life, then other stresses that might be present could also alter the subsurface maximum shear stress and thereby affect the rolling-element fatigue life of the component. The object of the work reported herein was to determine the effects that inner-ring press fit and centrifugal loading have on the fatigue life of the inner race of a roller bearing. This was accomplished by analyzing the subsurface stresses of the roller-bearing inner ring, including those due to press fit and ring rotation, and applying the results to a conventional bearing fatigue life analysis.

Analysis

Current evaluations of rolling-element fatigue life are based on either the orthogonal shear stress or the maximum shear stress (ref. 5) which occurs in a zone under the rolling-element contact surfaces. These shear stresses are a function of the contact (Hertz) stress due to two bodies in contact. The Hertzian stress, in turn, is a function of load, geometry, and material physical properties of the rolling-element bodies. Jones (ref. 6), on the basis of the work of Thomas and Hoersch (ref. 7), shows the principal stresses (see fig. 1) due to a Hertzian loading to be

$$\frac{\Delta X_X}{b} = -2\delta\left[\sqrt{1+\left(\frac{Z}{b}\right)^2} - \frac{Z}{b}\right] \tag{1}$$

$$\frac{\Delta Y_Y}{b} = -\frac{\left[\sqrt{1+\left(\frac{Z}{b}\right)^2} - \frac{Z}{b}\right]^2}{\sqrt{1+\left(\frac{Z}{b}\right)^2}} \tag{2}$$

$$\frac{\Delta Z_Z}{b} = -\frac{1}{\sqrt{1+\left(\frac{Z}{b}\right)^2}} \tag{3}$$

(Symbols are defined in the appendix.) Let $U=Z/b$ and $t=\sqrt{1+U^2}$; these equations become

$$\frac{\Delta X_X}{b} = -2\delta(t-U) \tag{4}$$

$$\frac{\Delta Y_Y}{b} = -\frac{(t-U)^2}{t} \tag{5}$$

$$\frac{\Delta Z_Z}{b} = -\frac{1}{t} \tag{6}$$

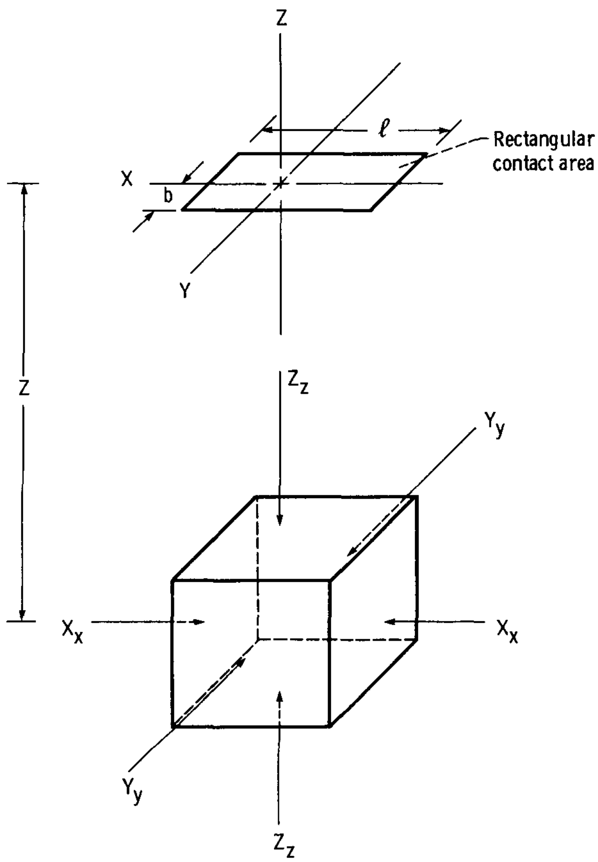

Figure 1.—Principal stresses on elementary subsurface particle at depth Z under Hertzian pressure area.

For roller bearings, the maximum shear stress is determined by the principal stresses in the Z-direction (direction of Hertzian loading) and the Y-direction (direction of rolling). Thus

$$\tau = \frac{1}{2}\left(Z_Z - Y_Y\right) \tag{7}$$

So, for Hertzian loading only, substituting from equations (5) and (6) into equation (7) gives

$$\tau = \frac{b}{\Lambda}\left(t - U - \frac{1}{t}\right) \tag{8}$$

But, from reference 6,

$$b^2 = \frac{P_o'(\theta_a + \theta_b)}{\pi l \Sigma\rho} \tag{9}$$

$$\left.\begin{aligned} \theta_a &= \frac{4\left(1-\delta_a^2\right)}{E_a} \\ \theta_b &= \frac{4\left(1-\delta_b^2\right)}{E_b} \end{aligned}\right\} \tag{10}$$

$$\Lambda = \left(\frac{1-\delta_a^2}{E_a} + \frac{1-\delta_b^2}{E_b}\right)\frac{2}{\Sigma\rho} \tag{11}$$

and

$$S_{max} = \frac{2P_o'}{\pi l b} \tag{12}$$

Let

$$E' = \frac{1-\delta_a^2}{E_a} + \frac{1-\delta_b^2}{E_b} \tag{13}$$

then

$$\theta_a + \theta_b = 4E' \tag{14}$$

$$\Lambda = \frac{2E'}{\Sigma\rho} \tag{15}$$

Equation (9) can now be written

$$b = \frac{2P_o'}{\pi l b}\,\frac{2E'}{\Sigma\rho} \tag{16}$$

or

$$b = S_{max}\Lambda \tag{17}$$

Substituting equation (17) into equation (8) gives

$$\tau = S_{max}\left(t - U - \frac{1}{t}\right) \tag{18}$$

Thus the shear stress, made nondimensional by the maximum Hertz stress, is a direct function of U, the depth below the surface, as shown in figure 2. A maximum value of the maximum shear stress occurs at a depth U of approximately 0.78. By taking the derivative of equation (18) with respect to U and setting the result equal to zero, one obtains

$$\frac{d\tau}{dU} = S_{max}\left(\frac{U}{t} + \frac{U}{t^3} - 1\right) = 0 \tag{19}$$

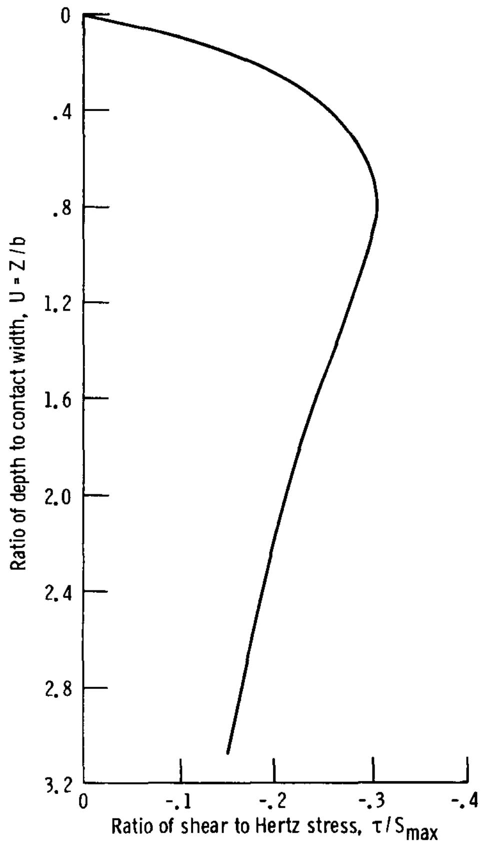

Figure 2.—Maximum shear stress as function of depth below surface for Hertzian loading. Stress on Z-axis below rectangular pressure area.

The solution to equation (19) is $U = 0.786152$, and the corresponding equation for the maximum shear stress becomes

$$\tau_{\max} = -0.30028\, S_{\max} \tag{20}$$

Equations (18) and (20) only account for the subsurface stresses due to the Hertzian contact and do not account for the effects of press fitting an inner ring on a shaft or for the effects of inner-ring speed. These effects can be accounted for through the method of superposition, by determining the values of subsurface stress in the Z- and Y-direction as a function of depth below the surface to correspond with equations (5) and (6).

Stresses Due to Press Fit

From reference 8, for the hoop stress we can write

$$(\sigma_h)_{\mathrm{PF}} = \frac{1}{r_o^2 - r_i^2}\left[r_i^2 P_i - r_o^2 P_o + \left(\frac{r_i r_o}{r}\right)^2 (P_i - P_o)\right] \tag{21}$$

Note that $P_o = 0$ and that P_i is due to a press fit of the ring on a shaft, that is,

$$P_i = \frac{\Delta}{r_i K_1} \tag{22}$$

Equation (21) can be written

$$(\sigma_h)_{\mathrm{PF}} = \frac{P_i r_i^2}{r_o^2 - r_i^2}\left[1 + \left(\frac{r_o}{r}\right)^2\right] \tag{23}$$

Similarly, for the radial stress we can write

$$(\sigma_r)_{\mathrm{PF}} = \frac{P_i r_i^2}{r_o^2 - r_i^2}\left[1 - \left(\frac{r_o}{r}\right)^2\right] \tag{24}$$

If we let

$$\left.\begin{aligned} \frac{r_i}{r_o} &= B \\ &\text{and} \\ \frac{r}{r_o} &= y \end{aligned}\right\} \tag{25}$$

equations (23) and (24) become

$$(\sigma_h)_{\mathrm{PF}} = \frac{P_i B^2}{1 - B^2}\left(1 + \frac{1}{y^2}\right) \tag{26}$$

$$(\sigma_r)_{\mathrm{PF}} = \frac{P_i B^2}{1 - B^2}\left(1 - \frac{1}{y^2}\right) \tag{27}$$

Stresses Due to Inner Ring Speed

From reference 8, for the hoop stress we can write

$$(\sigma_h)_{\mathrm{CF}} = \frac{3 - 2\nu}{8(1 - \nu)}\left(\frac{\gamma\omega^2}{g}\right)\left[r_o^2 + r_i^2 + \left(\frac{r_i r_o}{r}\right)^2 - r^2\left(\frac{1 - 2\nu}{3 - 2\nu}\right)\right] \tag{28}$$

Similarly, for the radial stress

$$(\sigma_r)_{\mathrm{CF}} = \frac{3 - 2\nu}{8(1 - \nu)}\left(\frac{\gamma\omega^2}{g}\right)\left[r_o^2 - r_i^2 - r^2 - \left(\frac{r_o r_i}{r}\right)^2\right] \tag{29}$$

Let

$$\left.\begin{aligned} K&=\frac{3-2\nu}{8(1-\nu)}\left(\frac{\gamma}{g}\right) \\ G&=\frac{1-2\nu}{3-2\nu} \end{aligned}\right\} \quad (30)$$

and use equation (25); equations (28) and (29) become

$$(\sigma_h)_{CF}=K\omega^2 r_o^2\left(1+B^2+\frac{B^2}{y^2}-Gy^2\right) \quad (31)$$

$$(\sigma_r)_{CF}=K\omega^2 r_o^2\left(1-B^2-\frac{B^2}{y^2}-y^2\right) \quad (32)$$

Combined Stress

By the method of superposition, the principal stresses in the Z- and Y-direction become

$$S_z=Z_Z+(\sigma_r)_{PF}+(\sigma_r)_{CF} \quad (33)$$

$$S_y=Y_Y+(\sigma_h)_{PF}+(\sigma_h)_{CF} \quad (34)$$

and the maximum shear stress is

$$\tau=\frac{1}{2}(S_z-S_y) \quad (35)$$

To utilize these equations, however, one must obtain the relation between U and y so that the stresses can all be determined at the same location.

From geometry (figs. 1 and 3)

$$r=r_o-Z=r_o-Ub \quad (36)$$

or

$$\frac{r}{r_o}=1-\frac{Ub}{r_o}=y \quad (37)$$

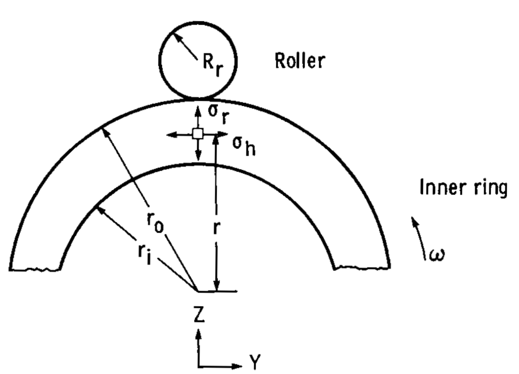

Figure 3.—Definition of geometric terms used in analysis of subsurface stress in roller-bearing inner ring.

and

$$U=\frac{r_o}{b}(1-y) \quad (38)$$

Substituting equation (17) gives

$$U=\frac{r_o}{S_{max}\Lambda}(1-y) \quad (39)$$

From figure 3

$$\Sigma\rho=\frac{1}{r_o}+\frac{1}{R_r}+\frac{1}{\infty}+\frac{1}{\infty}=\frac{R_r+r_o}{r_oR_r} \quad (40)$$

Substituting equation (40) into equation (15) gives

$$\Lambda=\frac{2E'r_oR_r}{r_o+R_r} \quad (41)$$

Using equation (41) in equation (39) results in

$$U=\frac{\frac{r_o}{R_r}+1}{2S_{max}E'}(1-y) \quad (42)$$

or

$$U=\frac{R'+1}{2S_{max}E'}(1-y) \quad (43)$$

where

$$R'=\frac{r_o}{R_r} \quad (44)$$

For simplicity, let

$$K_2=\frac{R'+1}{2S_{max}E'} \quad (45)$$

then

$$U=K_2(1-y) \quad (46)$$

Proper substitution of equations (33) and (34) into equation (35) by using equations (5), (6), (26), (27), (31), and (32) along with equation (17) leads to an expression for the maximum shear stress as a function of depth below a Hertzian contact that accounts for both ring press fit and ring speed:

$$\tau = S_{max}\left(t - U - \frac{1}{t}\right) - (m + AB^2)\frac{1}{y^2} + \frac{A}{2}(G-1)y^2 - AB^2 \qquad (47)$$

where, for simplicity

$$m = \frac{P_i B^2}{1 - B^2}$$

$$A = K\omega^2 r_o^2 \qquad (48)$$

Again, taking the derivative of equation (47) with respect to y and setting the result equal to zero lead to the value of y where the shear stress is a maximum. Using the chain rule that $dS/dy = (dS/dU)\ (dU/dy)$ gives

$$\frac{d\tau}{dy} = -S_{max}K_2\left(\frac{U}{t} + \frac{U}{t^3} - 1\right) + \frac{2(m + AB^2)}{y^3} + A(G-1)y = 0 \qquad (49)$$

Results and Discussion

The relative values of subsurface stress are shown in figure 4 for the typical roller-bearing inner-ring data given in table I. The principal stress in the Z-direction is shown in figure 4(a), while the principal stress in the Y-direction is shown in figure 4(b). The stress is nondimensionalized by the Hertz stress S_{max}. Note that $y = 0.90$ is the inner radius, $y = 1$ is the outer radius of the ring, and the ring was considered flangeless.

In figure 4(a), the stress due to ring speed is the largest component at the inner surface, but the subsurface compressive stress due to the Hertzian loading becomes dominant as the outer (contact) surface is approached. In figure 4(b), the stress due to ring speed is again the largest at the inner surface, and the stress from the press fit is influential. Note that the ring speed is high in the example problem and that the pressure assumed for the press fit is probably moderate. Again, however, the compressive stress due to the Hertzian loading becomes dominant as the outer surface is approached. The principal stress Sy does remain tensile (positive) until about $y = 0.997$, which will influence the maximum shear stress.

When the principal stresses from figure 4 are combined in accordance with equation (35), the result is the maximum shear stress (fig. 5). To observe the change in the maximum shear stress when the effects of ring press fit and ring speed are added, the results in figure 5 can be compared with those due to Hertzian loading only (fig. 2). This is shown in figure 6, where the contributions to the maximum shear stress are shown separately. The increase in maximum value of the maximum shear stress for this example is about 33 percent. The solution to equation (49)

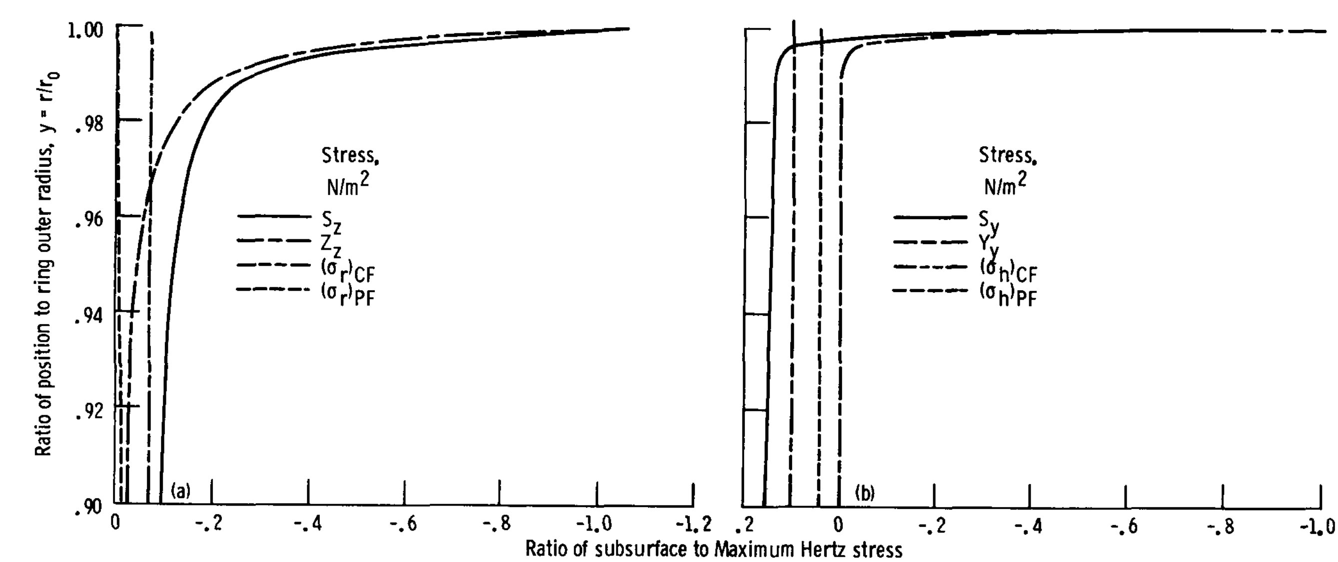

(a) In radial, or Z-, direction; $S_z = Z_z + (\sigma_r)_{PF} + (\sigma_r)_{CF}$ (eq. (33)).
(b) In hoop, or Y-, direction; $S_y = Y_y + (\sigma_h)_{PF} + (\sigma_h)_{CF}$ (eq. (34)).

Figure 4.—Components of subsurface stress in roller-bearing inner ring for conditions described in table I.

TABLE I.—VALUES FOR EXAMPLE PROBLEM

(a) Variables

B	0.90
P_i, N/m² (ksi)	6.89×10^6 (1)
ω, rad/sec (rpm)	2000 (19 000)
r_o, mm (in)	63.5 (2.5)
R'	10
S_{max}, N/m² (ksi)	1.379×10^9 (200)

(b) Constants

K for steel, N-sec²/m⁴ (lb-sec²/in⁴)	3352 (3.14×10^{-4})
G	0.1667
E', m²/N (in²/lb)	9.11×10^{-12} (6.28×10^{-8})

for this example is $y=0.998204$ ($U=0.786465$), where $\tau_{max}=-0.402\ S_{max}$. The depth to the maximum shear stress changed only very slightly from that of the Hertz loading only.

The rolling-element fatigue life is taken to be inversely proportional to the maximum shear stress to the ninth power (ref. 9). Therefore, if we define a life ratio LR as the ratio of fatigue life based on the maximum shear stress that included the effects of ring speed and press fit to the fatigue life based on the maximum shear stress from the Hertzian loading only, we can write

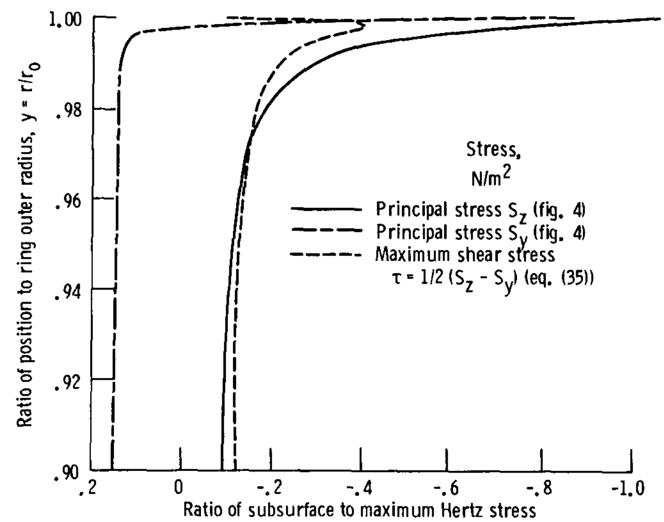

Figure 5.—Principal and maximum shear stresses in roller-bearing inner ring for conditions described in table I.

$$LR=\frac{L_T}{L_H}=\left(\frac{\tau_{max,H}}{\tau_{max,T}}\right)^9 \tag{50}$$

Here $\tau_{max,H}$ is obtained from equation (20) and $\tau_{max,T}$ is obtained from equation (47), by using the value of y obtained from equation (49).

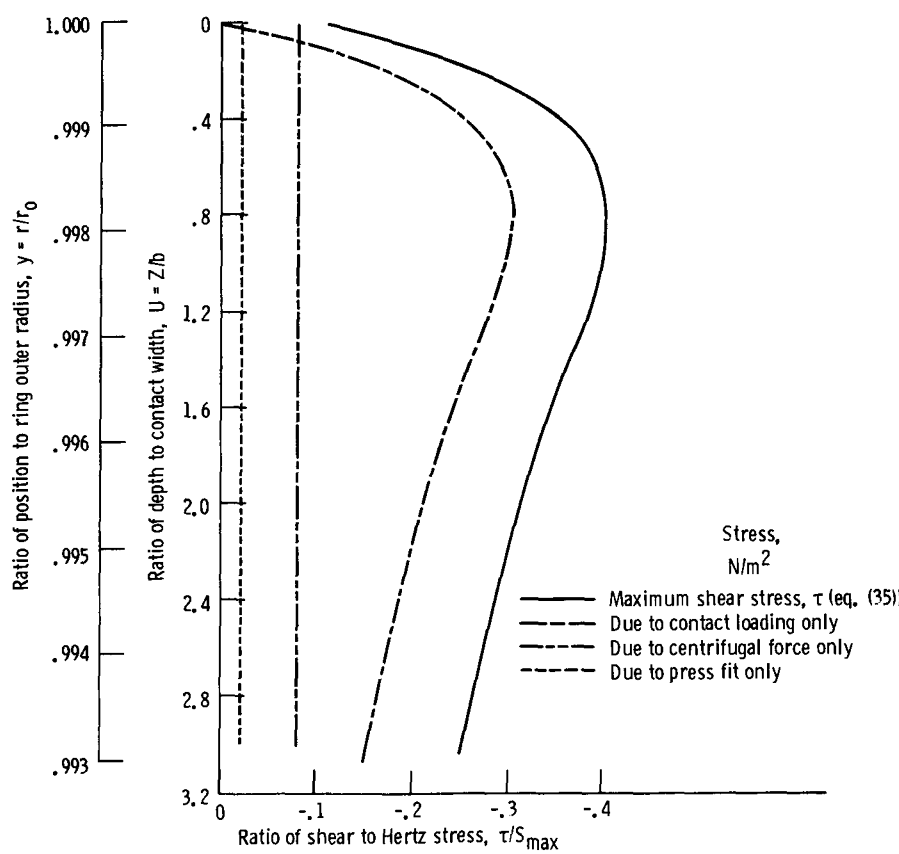

Figure 6.—Components of maximum shear stress in roller-bearing inner ring for conditions described in table I.

For the example the value of LR, which is a measure of the effects of press fit and ring speed, is

$$LR = \left(\frac{-0.30028 \times 1.4 \times 10^9}{-0.40167 \times 1.4 \times 10^9} \right)^9 = 0.0729$$

That is, the corrected life is only 0.07 times that calculated by using stresses from the Hertzian loading only.

To observe these effects over a broader range of variables, equations (47) and (49) were used to calculate LR (eq. (50)) for the following conditions: ring thicknesses B, 0.5 to 0.92; Hertz stress, 0.69 to 2.07 GPa (100 to 300 ksi); ring speed, 500 and 2000 rad/sec (4800 and 19 000 rpm); ring outer radius, 25.4 and 63.5 mm (1 and 2.5 in); press fit pressure, 6.9×10^6 N/m^2 (1 ksi); radius ratio R', 5 and 10. The results are shown in figures 7 to 10.

For a ring with an outer radius of 63.5 mm (2.5 in) figure 7 shows that the relative influence of press fit and ring speed on fatigue life diminishes as the Hertz stress is increased, as the ring becomes thicker, or as the ring speed is decreased. Figure 8 shows the same data plotted against radius ratio. Several calculations for the conditions of figure 7 were made with $R' = 5$, and the life ratio results were the same. Increasing the press fit

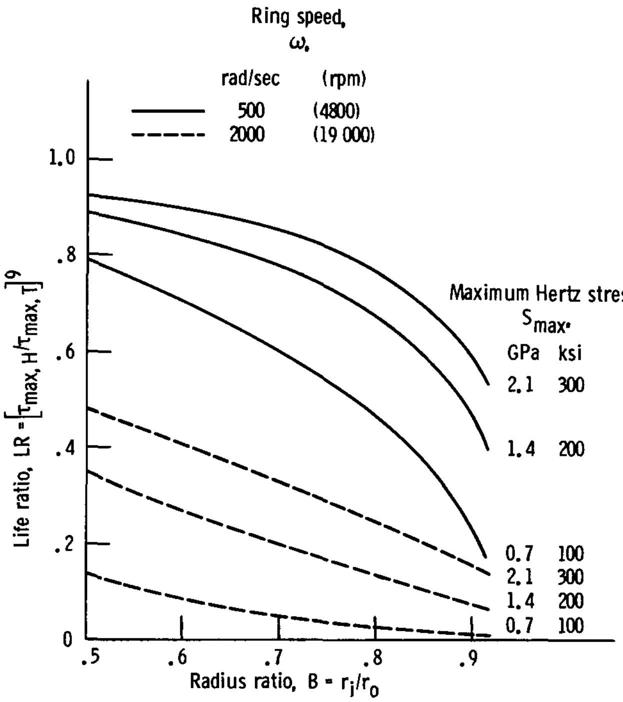

Figure 8.—Life ratio as function of radius ratio for three maximum Hertz stresses and two ring speeds; $r_o = 63.5$ mm (2.5 in); $P_i = 6.9 \times 10^6$ N/m^2 (1 ksi); $R' = 10$.

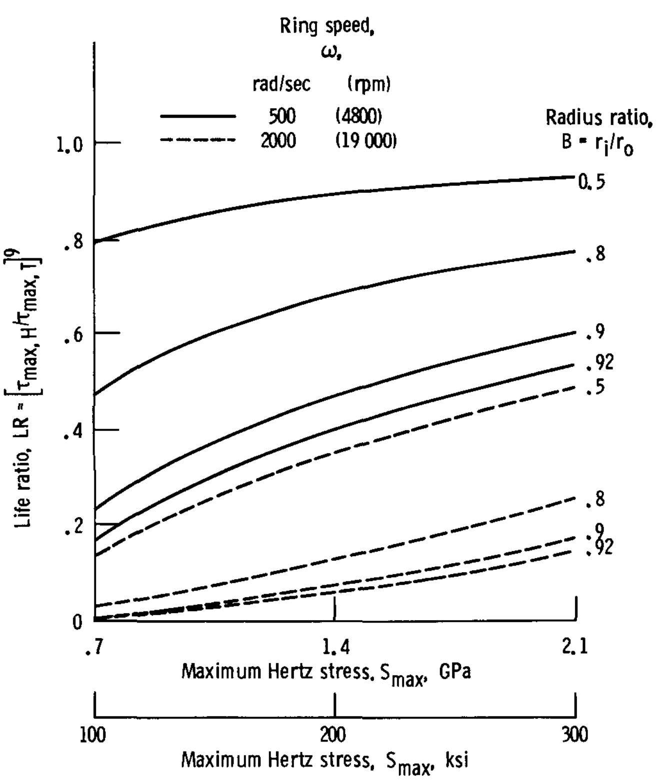

Figure 7.—Life ratio as function of Hertz stress for four ring thicknesses and two ring speeds. $r_o = 63.5$ mm (2.5 in); $P_i = 6.9 \times 10^6$ N/m^2 (1 ksi); $R' = 10$.

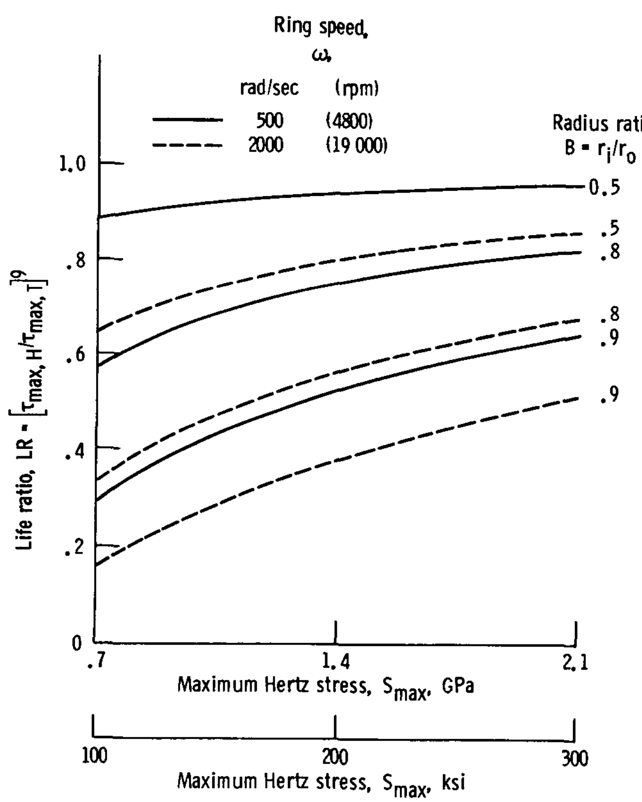

Figure 9.—Life ratio as function of Hertz stress for three ring thicknesses and two ring speeds. $r_o = 25.4$ mm (1.0 in); $P_i = 6.9 \times 10^6$ N/m^2 (1 ksi); $R' = 5$.

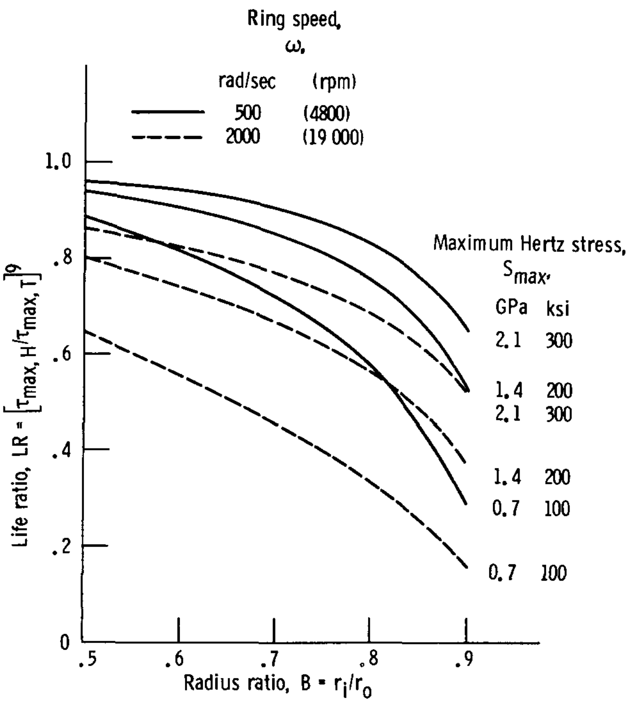

Figure 10.—Life ratio as function of radius ratio for three Hertz stresses and two ring speeds. $r_o = 25.4$ mm (1.0 in); $P_i = 6.9 \times 10^6$ N/m^2 (1 ksi); $R' = 5$.

pressure would lower the values of *LR*. The pressure used in figures 7 and 8 represents an interference fit of about 0.051 mm (0.002 in) on the diameter.

Figures 9 and 10 show the results obtained for an outer radius of 25.4 mm (1.0 in) and an R' of 5. Here also the life ratio results with an R' of 10 were the same. A comparison of figures 7 and 9 shows that the life ratios with the smaller outer radius were generally higher than for the corresponding larger ring and were not so influenced by ring speed.

Since there are many values of *LR* of 0.5 or less, it may be concluded that the press fit and loading due to ring speed can have a significant effect on the fatigue life calculated for an inner-ring contact.

Summary of Results

An analysis was performed to determine the effects of speed and press fit on the rolling-element fatigue life of a roller-bearing inner-ring contact. The maximum shear stresses below the Hertzian contact were analyzed and applied to a fatigue life analysis for a roller-bearing inner ring having outer diameters of 51 and 127 mm (2.0 and 5.0 in) and inner- to outer-diameter ratios of 0.50 to 0.92 run at speeds of 500 and 2000 rad/sec. The following results were obtained:

1. The combined effects of speed and press fit of a roller-bearing inner ring can reduce the fatigue life in excess of 90 percent from conventional life calculations.
2. Centrifugal force effects can account for 80 percent of the reduction in life at the higher speed. At the lower speed, press fit can account for 80 percent of the (lower) life reduction.
3. The depth to the maximum shear stress remains relatively unchanged by speed and press fit, over the range calculated, from that established by conventional theory.

National Aeronautics and Space Administration
Lewis Research Center
Cleveland, Ohio, May 17, 1985

Appendix—Symbols

A defined by eq. (48), N/m^2 (lb/in^2)

B defined by eq. (25), dimensionless

b semiwidth of contact area (see fig. 1), m (in)

E modulus of elasticity, N/m^2 (lb/in^2)

E' defined by eq. (13), m^2/N (in^2/lb)

G defined by eq. (30), dimensionless

g gravitational constant, m/sec^2 (in/sec^2)

K defined by eq. (30), $N\text{-}sec/m^4$ ($lb\text{-}sec/in^4$)

K_1 constant relating press fit to pressure, ($2/E(1-B^2)$ for a solid shaft of same material)

K_2 defined by eq. (45), dimensionless

L contact fatigue life, hr

LR life ratio, defined by eq. (50)

l length of contact area (fig. 1), m (in)

m defined by eq. (48), N/m^2 (lb/in^2)

P_i pressure on r_i due to press fit, N/m^2 (lb/in^2)

P_o pressure on r_o, N/m^2 (lb/in^2)

P_o' roller load, N (lb)

R radius of curvature, m (in)

R_r radius of roller (fig. 3), m (in)

R' ratio, defined by eq. (44), dimensionless

r radius to element (fig. 3), m (in)

r_i ring inner radius (fig. 3), m (in)

r_o ring outer radius (fig. 3), m (in)

S_{max} Hertz stress at center of contact, N/m^2 (lb/in^2)

S_y principal stress in Y-direction (eq. (34)), N/m^2 (lb/in^2)

S_z principal stress in Z-direction (eq. (33)), N/m^2 (lb/in^2)

t simplifying term, $\sqrt{1+U^2}$

U dimensionless depth below surface, Z/b

X axis perpendicular to rolling direction

X_x principal stress in X-direction, Hertz loading only (eq. (4)), N/m^2 (lb/in^2)

Y axis in direction of rolling

Y_Y principal stress in Y-direction, Hertz loading only (eq. (5)), N/m^2 (lb/in^2)

y defined by eq. (25), dimensionless

y_{max} value of y at τ_{max}, dimensionless

Z distance below Hertz contact surface (fig. 1), m (in), or axis in direction of Hertzian loading

Z_Z principal stress in Z-direction, Hertz loading only (eq. (6)), N/m^2 (lb/in^2)

γ density of material, N/m^3 (lb/in^3)

Δ press fit on radius, m (in)

δ,ν Poisson's ratio, dimensionless

θ defined by eq. (10), m^2/N (in^2/lb)

Λ defined by eq. (15), m^3/N (in^3/lb)

$\Sigma\rho$ curvature sum, $1/R_a + 1/R_b$, 1/m (1/in)

σ stress, N/m^2 (lb/in^2)

τ maximum shear stress, N/m^2 (lb/in^2)

τ_{max} maximum value of τ, N/m^2 (lb/in^2)

ω inner-ring speed, rad/sec

Subscripts:

a body a

b body b

CF due to inner-ring speed

H based on Hertz loading only

h hoop, or Y-, direction

PF due to press fit on inner ring

r radial, or Z-, direction

T based on press fit, ring speed, and Hertz loading

References

1. Scott, R.L.; Kepple, R.K.; and Miller, M.H.: The Effect of Processing-induced Near-surface Residual Stress on Ball Bearing Fatigue. Rolling Contact Phenomena, Joseph B. Bidwell, ed., Elsevier, 1962, pp. 301-316.
2. Zaretsky, Erwin V., et al: Effect of Component Differential Hardnesses on Residual Stress and Rolling-Contact Fatigue. NASA TN-D-2664, 1965.
3. Almen, J.O.: Effects of Residual Stress on Rolling Bodies. In Rolling Contact Phenomena, Jospeh B. Bidwell, ed., Elsevier, 1962, pp. 400–424.
4. Townsend, Dennis P.; and Zaretsky, Erwin V.: Effect of Shot Peening on Surface Fatigue Life of Carburized and Hardened AISI 9310 Spur Gears. NASA TP-2047, 1982.
5. Harris, T.A.: Rolling Bearing Analyses. Second ed., John Wiley and Sons, New York, 1984.
6. Jones, A.B.: New Departure—Analysis of Stress and Deflections, Vol. I. New Departure Div., General Motors Corp, 1946.
7. Thomas, Howard R.; and Hoersch, Victor A.: Stresses due to the Pressure of One Elastic Solid on Another. Bulletin No. 212, Engineering Experiment Station, University of Illinois, July 1930.
8. Faupel, J.H.: Engineering Design. John Wiley and Sons, 1964.
9. Lundberg, G.; and Palmgren, A.: Dynamic Capacity of Rolling Bearings. Acta Polytech. Mech. Eng. Ser., vol. 1, no. 3, 1947.

1. Report No.	2. Government Accession No.	3. Recipient's Catalog No.
NASA TP-2496		

4. Title and Subtitle Effect of Speed and Press Fit on Fatigue Life of Roller-Bearing Inner-Race Contact	5. Report Date July 1985
	6. Performing Organization Code 505-33-7C
7. Author(s) Harold H. Coe and Erwin V. Zaretsky	8. Performing Organization Report No. E-2476
	10. Work Unit No.
9. Performing Organization Name and Address National Aeronautics and Space Administration Lewis Research Center Cleveland, Ohio 44135	11. Contract or Grant No.
	13. Type of Report and Period Covered Technical Paper
12. Sponsoring Agency Name and Address National Aeronautics and Space Administration Washington, D.C. 20546	14. Sponsoring Agency Code

15. Supplementary Notes

16. Abstract

An analysis was performed to determine the effects of inner-ring speed and press fit on the rolling-element fatigue life of a roller-bearing inner-race contact. The effects of the resultant hoop and radial stresses on the principal stresses were considered. The maximum shear stresses below the Hertzian contact were determined for different conditions of inner-ring speed, load, and geometry and were applied to a conventional ring life analysis. The race-contact fatigue life was reduced by more than 90 percent for some conditions when speed and press fit were considered. The depth of the maximum shear stress remained virtually unchanged.

17. Key Words (Suggested by Author(s))	18. Distribution Statement
Fatigue life; High-speed bearings; Roller-element bearings; Subsurface stress; Hoop stress; Press fit	Unclassified - unlimited STAR Category 37

19. Security Classif. (of this report)	20. Security Classif. (of this page)	21. No. of pages	22. Price*
Unclassified	Unclassified	12	A02

*For sale by the National Technical Information Service, Springfield, Virginia 22161

NASA-Langley, 1985